

Experimental and Theoretical Study of Aromatic–Aromatic Interactions. Association Enthalpies and Central and Distributed Multipole Electric Moments Analysis

Silvia Pérez-Casas,^{*,†} Jesús Hernández-Trujillo,^{*,‡} and Miguel Costas^{*,†}

Facultad de Química, Universidad Nacional Autónoma de México, Cd. Universitaria, México D.F. 04510, México

Received: December 12, 2002; In Final Form: February 6, 2003

Aromatic–aromatic interactions are studied experimentally through heat capacity measurements that, with the aid of an association model, provide an estimate of the association enthalpy of the aromatic–aromatic complexes formed in solution. These enthalpies are empirically correlated with the product of the quadrupole moments of the molecules involved. The compounds used in this work are hexafluorobenzene (HFB), pentafluorobenzene (PFB), trifluorobenzene (TFB), fluorene (FB), benzene (BEN), toluene (TOL), naphthalene (NAP), and 1-methylnaphthalene (MEN). The 10 pairs studied are HFB–MEN, HFB–BEN, HFB–TOL, NAP–HFB, PFB–MEN, PFB–BEN, HFB–FB, BEN–MEN, FB–MEN, and TFB–MEN. The electrostatic interaction between the molecules forming the 10 aromatic–aromatic pairs is calculated expressing their charge distributions in terms of both central and distributed multipole electric moments. It is concluded that the changes in association enthalpies of aromatic–aromatic complexes can be explained by the electrostatic contribution to the interaction energy.

I. Introduction

Aromatic–aromatic interactions have been shown to play an important role in the properties of many systems in chemistry, biochemistry, and material science.¹ For this reason, they have been the subject of numerous reports at both the experimental and theoretical levels. Often, these interactions occur between parts of complicated molecules as in the cases of many host–guest systems² and proteins, where aromatic–aromatic interactions have been suggested to be important in the stabilization of their tertiary structure.³ In these kinds of systems, it is difficult to isolate the role played by the aromatic–aromatic interactions from the many others present, and hence, it is useful to examine simple mixtures. It is in this context that in the present work we study, at the experimental and theoretical levels, a series of mixtures where interactions between aromatic molecules are present.

At the experimental level, solid–liquid phase equilibria measurements for binary mixtures composed of an aromatic hydrocarbon and an aromatic fluorocarbon have shown the existence of 1:1 complexes in the solid state. These complexes melt at a considerable higher temperature than the pure components, e.g., 19° in the case of hexafluorobenzene mixed with benzene⁴ and approximately 100° in the case of hexafluorobenzene mixed with 1-methylnaphthalene.⁵ The solid–liquid phase diagrams for other binary mixtures⁶ such as hexafluorobenzene mixed with toluene, with *p*-xylene, and with mesitylene display a similar behavior. The hexafluorobenzene–benzene complex, by far the most studied one, has been characterized by X-ray diffraction and D and ¹³C NMR.⁷ It was concluded that the crystal structure consists of molecular pairs packed in a face-to-face manner and that the interaction between

the two molecules is of a relatively weak nature. This complex has also been studied using optical heterodyne-detected Raman-induced Kerr effect spectroscopy.⁸ In the liquid state, the existence of these complexes was suggested long ago on the basis of thermodynamic data⁹ which indicated that for these aromatic fluorocarbon + aromatic hydrocarbon mixtures the excess Gibbs energies G^E and the excess enthalpies H^E are negative and the excess heat capacities C_p^E are positive. Detailed neutron and X-ray diffraction studies of the hexafluorobenzene–benzene mixture¹⁰ confirmed the presence of the 1:1 complex in the liquid state and suggested a reorientation from the mutually perpendicular geometry in the pure components to a parallel alignment of the molecules in the complex. Among several thermodynamic quantities, the heat capacity has proven to be a good sensor of structure in liquid mixtures. It has been employed as a useful tool for studying the self-association of many types of alcohols¹¹ and the formation of alcohol–proton acceptor complexes.¹² In these cases, complexation takes place through the formation of H bonds, an interaction which is stronger than that between aromatic molecules. However, as it will be seen in detail below, using ternary mixtures of the type A + (B + I), where A and B are the aromatic compounds and I is an inert solvent (*n*-alkane), it is possible to study the A–B weak interaction. In this work, we have measured heat capacities for 10 A–B pairs with A and B being chosen such that their dipole moments are zero or small and they have widely different quadrupole moments, ranging from large positive to large negative values. From these experimental data, the enthalpies and equilibrium constants for the formation of the AB complexes were obtained using an extension^{11,12} of the association model due to Treszczanowicz and Kehiaian (TK).¹³

The interactions between aromatic molecules have also been the subject of numerous theoretical reports. A simple electrostatic model has been invoked for the interpretation of a number of experiments where interactions between aromatic molecules

* To whom correspondence should be addressed. E-mail: silpeca@servidor.unam.mx (S.P.-C.); jesus.hernandez@correo.unam.mx (J.H.-T.); costasmi@servidor.unam.mx (M.C.).

[†] Laboratorio de Termofísica, Departamento de Fisicoquímica.

[‡] Departamento de Física y Química Teórica.

are involved.^{14–16} For example, both the crystal structure of the 1:1 hexafluorobenzene–benzene solid binary mixture and the hexafluorobenzene–1-methylnaphthalene solid–liquid diagram have been interpreted in terms of the interactions between the permanent quadrupole moments of the molecules involved in each case. The same explanation has been given to the local structure found for the 1:1 hexafluorobenzene–benzene binary mixture in the liquid state. A quantum mechanical study of the hexafluorobenzene–benzene and hexafluorobenzene–fluorobenzene dimers led to conclude that dispersion interactions are also important in these systems.¹⁷ For both dimers, it was concluded that at the Hartree–Fock (HF) level it is not possible to find a reliable minimum in the interaction energy curve, and for the proper description of the interaction, the inclusion of electron correlation is needed (at the MP2 level in that work). In addition, ref 17 concluded that it is the electrostatic contribution which determines the difference in stability between the different dimers, in agreement with the model based solely on central quadrupole moments. For this reason, apart from the possibility of performing ab initio supermolecule calculations, a reliable classical electrostatic interaction model is of great interest. The electrostatic interaction between two molecules can be computed in a number of ways. The charge distribution representing each of the interacting molecules can be expressed in terms of either a single set of multipole moments (central multipole moments) or an arbitrary number of them (distributed multipole moments), located at selected positions in space. The later choice has been proved to be more accurate, even if only a finite number of terms of the perturbation expansion for the interaction energy are included. The distributed multipole moments can be obtained from quantum-mechanical calculations under different assumptions. In this work, we used two of them, namely, Stone's multipole analysis^{18,19} and the theory of atoms in molecules.²⁰ Both approaches have been used in the past for the calculation of intermolecular interactions.^{15,16,21–24} Employing these theoretical tools and using a simple interaction model, we explored the role of the electrostatic interaction on the observed experimental enthalpies of aromatic–aromatic complex formation.

II. Experimental Section

The aromatic compounds studied in this work were hexafluorobenzene (HFB), pentafluorobenzene (PFB), trifluorobenzene (TFB), fluorene (FB), benzene (BEN), toluene (TOL), naphthalene (NAP), and 1-methylnaphthalene (MEN). The inert (I) solvent used was *n*-heptane (*n*-C₇). All materials were from Aldrich Chemical Co. with stated purities between 99 and 99.9% and were used without further purification. The 10 A–B pairs studied were HFB–MEN, HFB–BEN, HFB–TOL, NAP–HFB, PFB–MEN, PFB–BEN, HFB–FB, BEN–MEN, FB–MEN, and TFB–MEN.

Apparent molar heat capacities of the aromatic compound A, $\phi_{C,A}$, were determined in mixtures of the type A + (*p* wt % B + *n*-C₇) at 298.15 K; here, *p* denotes the weight percent of B in the binary (B + I). Measurements were made for different *p* values as a function of the concentration of A (from extreme dilution up to c.a 5 wt %). To obtain the associational part of the apparent molar heat capacities (see below for details), $\phi_{C,A}$ at 298.15 K was also measured in the binaries (A + I) as a function of A concentration. Volumetric heat capacities were measured using a Picker flow microcalorimeter (Sodev Inc., Canada). The instrumentation and procedures have been described in the literature.²⁵ These volumetric heat capacities were converted into molar heat capacities by determining the density

of each mixture. Density data were obtained with a vibrating-cell densimeter (Sodev Inc., Canada), using *n*-C₇ ($\rho = 0.679\,46\text{ g cm}^{-3}$ from ref 26) and carbon tetrachloride ($\rho = 1.584\,36\text{ g cm}^{-3}$ from ref 26) as references. Solutions were prepared by weight, and extreme care was taken during their preparation and handling in order to minimize evaporation losses. Depending on the concentration range, the heat capacity of each solution was determined using as a reference either *n*-C₇ ($C_p^o = 224.98\text{ J K}^{-1}\text{ mol}^{-1}$ from ref 26) or the previous less concentrated solution. The apparent molar heat capacities of component A were calculated using

$$\phi_{C,A} = (C_p^{\text{soln}} - x^+ C_p^+)/x_A \quad (1)$$

where C_p^+ and x^+ are the heat capacity and the mole fraction ($x_A + x^+ = 1$) of the solvent, i.e., *n*-C₇ for the (A + I) mixtures or the binary solution (B + I) for the A + (B + I) solutions, respectively. The associational part of the apparent molar heat capacity of A was obtained as

$$\phi_{C,A}(\text{assoc}) = \phi_{C,A} - \lim \phi_C^b(x_A \rightarrow 0) \quad (2)$$

where $\phi_{C,A}$ is given by eq 1 and $\lim \phi_C^b$ is the infinite-dilution value of the apparent heat capacity of A in the (A + I) binary mixture. From eq 2, the infinite-dilution value of the association part of the apparent molar heat capacity of A in the ternary A + (B + I) mixtures is

$$\lim \phi_{C,A}(\text{assoc})(x_A \rightarrow 0) = \lim \phi_{C,A}(x_A \rightarrow 0) - \lim \phi_C^b(x_A \rightarrow 0) \quad (3)$$

The accuracy was $\pm 1 \times 10^{-5}\text{ g cm}^{-3}$ for the density and $\pm 1 \times 10^{-4}\text{ J K}^{-1}\text{ cm}^{-3}$ for the volumetric heat capacities. Through repetition of the present measurements, the accuracy on $\phi_{C,A}$ appears to be $\pm 2\text{ J K}^{-1}\text{ mol}^{-1}$ for the most diluted solutions.

III. Calculation of Multiple Moments and of Electrostatic Interactions

The calculation of the electrostatic interaction energy, E_{elec} , as a multipole expansion involves appropriate consideration of both its convergence properties and the source of electric moments used. The convergence properties of the expansion have been studied by a number of authors. Stone and collaborators^{18,19} expanded the moments of the electron density on a Gaussian basis set. Using the properties of the spherical harmonics, the central multipole moments of a charge distribution are partitioned into an arbitrary number of sets, referred to chosen locations in space as for example the nuclear positions. The convergence properties of this expansion are greatly improved when the number of expansion centers is enlarged, i.e., when a set of distributed moments are used.¹⁹ This approach has been applied to several specific problems, including some aromatic–aromatic interactions,^{15,16,23} where satisfactory agreement with available experimental data was achieved. A more fundamental approach for the partition of the moments of an electron distribution is provided by the theory of atoms in molecules (AIM).²⁰ In this theory, real space is partitioned into nonoverlapping subsets, providing a quantum-mechanical definition of an atom in a molecule. The properties of the atoms thus defined can be computed as the average values of the corresponding quantum operators. In particular, recent studies on the properties of electrostatic potentials²⁷ and interaction energies^{24,28} expanded in terms of AIM distributed multipole moments have demonstrated the appropriateness of their use.

In this work, we performed quantum-chemical calculations of the electric moments of the aromatic molecules involved in the molecular pairs studied. Only up to quadrupole moments were included in the interaction model. Several reports have dealt with the calculation of central electric moments of substituted benzenes. In particular, it has been reported²⁹ that quadrupole moments of halobenzenes at the HF/6-31G** level are in reasonable agreement with experimental data. Further improvement could be achieved if electron correlation is included. Nevertheless, for the purposes of the present work, the basic features of the electron density of the interacting molecules are well recovered at the HF approximation. For the calculation of E_{elec} , the HF/6-31G** level of theory was selected to compute the multipole moments, either central or distributed (Stone or AIM). For all of the molecules, except MEN for which an ab initio molecular geometry was used,³⁰ experimental geometries were employed.³¹ Central and Stone distributed multipole moments were computed using CADPAC,³² whereas AIM multipole moments were calculated with the AIMPAC³³ set of programs using wave functions obtained from Gaussian 94.³⁴

The electrostatic interaction energies were computed using a Fowler-Buckingham type pair-potential²² where the short-range part of the interaction is of the hard-spheres type. In this work, the long-range part of the interaction comprises only the electrostatic contribution. The perturbation expansion for E_{elec} includes terms for the interaction between sites a and b on molecules A and B, respectively, of the form³⁵

$$E_{\text{elec}}^{ab} = Tq^a q^b + T_i(q_i^a \mu_i^b - q^b \mu_i^a) + \frac{1}{3}T_{ij}(q^a \Theta_{ij}^b + q^b \Theta_{ij}^a) - T_{ij}\mu_i^a \mu_j^b - \frac{1}{3}T_{ijk}(\mu_i^a \Theta_{jk}^b - \mu_i^b \Theta_{jk}^a) + T_{ijkl}\frac{1}{9}\Theta_{ij}^a \Theta_{kl}^b + \dots \quad (4)$$

where Einstein notation has been used and q , μ and Θ are the charge, dipole moment vector and quadrupole moment tensor, respectively. The T -tensors are defined as

$$T = (4\pi\epsilon_0)^{-1} R^{-1}, T_i = -(4\pi\epsilon_0)^{-1} R_i R^{-3}, T_{ij} = (4\pi\epsilon_0)^{-1} (3R_i R_j - R^2 \delta_{ij}) R^{-5} \\ T_{ijk} = (4\pi\epsilon_0)^{-1} (-3)[5R_i R_j R_k - R^2(R_i \delta_{jk} + R_j \delta_{ki} + R_k \delta_{ij})] R^{-7} \\ T_{ijkl} = (4\pi\epsilon_0)^{-1} [35R_i R_j R_k R_l - 5R^2(R_i R_j \delta_{kl} + R_i R_k \delta_{jl} + R_i R_l \delta_{jk} + R_j R_k \delta_{il} + R_j R_l \delta_{ik} + R_k R_l \delta_{ij}) + R^4(\delta_{ij} \delta_{kl} + \delta_{ik} \delta_{jl} + \delta_{il} \delta_{jk})] R^{-9} \quad (5)$$

with R_i being the i th component of the vector from site A to site B. Terms in eq 4 are the charge–charge, charge–dipole, ..., and quadrupole–quadrupole contributions to E_{elec} , respectively. In the case of central moments, they are referred to the center of mass whereas the distributed moments are located at the nuclear positions. Only the first nonzero moment of a charge distribution is origin independent. As a consequence, only E_{elec} and its lowest order nonzero-contribution are suitable of a direct physical interpretation. In the case of the interaction between nondipolar aromatic molecules, a model based on central quadrupole moments describes the interaction. In the case of distributed multipole moments, charge–charge contributions are important and quadrupole–quadrupole terms are only a minor fraction of E_{elec} . Such is the case of the BEN–BEN and BEN–HFB dimers where the quadrupole–quadrupole contribution is

TABLE 1: Infinite-Dilution Apparent Molar Heat Capacities, $\lim \phi_{C,A}^b(x_A \rightarrow 0)$, for Aromatic Compounds in n -Heptane, Pure Component Heat Capacities, C_p^o , and Calculated Quadrupole Moments, Q^a

aromatic	$\lim \phi_{C,A}^b(x_A \rightarrow 0)^b$ J K ⁻¹ mol ⁻¹	C_p^o ^c J K ⁻¹ mol ⁻¹	Q Buckingham
HFB	213.9 ± 0.3	221.6	9.69
PFB	198.8 ± 0.6	204.7	7.17
TFB	171.9 ± 0.3		0.92
FB	141.1 ± 0.8	146.4	−6.25
BEN	125.6 ± 0.8	135.8	−8.54
NAP	190.6 ± 2.1		−13.37
MEN	222.9 ± 0.3	224.4	−12.94
TOL	152.4 ± 0.2	157.1	−8.00

^a Heat capacity values are at 298.15 K. ^b From a linear fit of the $\phi_{C,A}$ vs aromatic compound concentration data. ^c From ref 42.

only relevant in a model that uses central moments. That this contribution is negligible using distributed moments suggests that including terms up to quadrupole–quadrupole in eq 4 could suffice to obtain reasonable values for E_{elec} of aromatic–aromatic interactions.

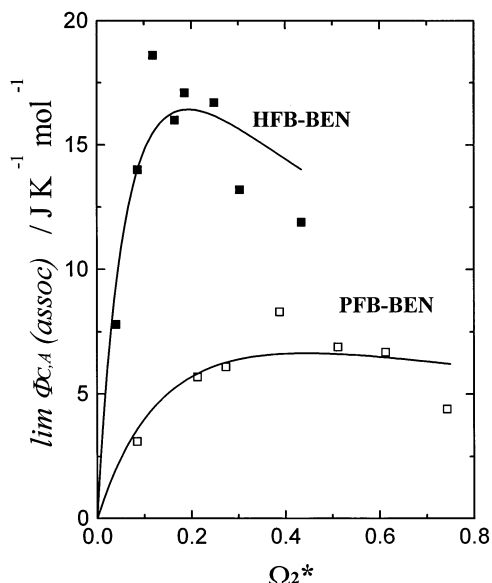
IV. Results and Discussion

In the concentration range studied, the apparent heat capacities from eq 1 vary linearly with the concentration of A both in the mixtures A + I and A + (B + I). Table 1 reports $\lim \phi_{C,A}^b(x_A \rightarrow 0)$ for the binaries A + I, and Table 2 displays $\lim \phi_{C,A}(x_A \rightarrow 0)$ as a function of p , for the A + (B + I) ternary mixtures. The experimental $\lim \phi_{C,A}(\text{assoc})(x_A \rightarrow 0)$ for HFB plotted against Ω^*_2 , the volume fraction of BEN in the binary (BEN + n -C₇), are shown in Figure 1. These limiting apparent molar heat capacities were obtained using eq 3 with the data reported in Tables 1 and 2 and represent the situation where an isolated HFB molecule is surrounded by (BEN + n -C₇) binary mixtures of different concentrations. As BEN concentration increases, $\lim \phi_{C,A}(\text{assoc})(x_A \rightarrow 0)$ rises up rapidly, passes through a maximum and then decreases. The increase in $\lim \phi_{C,A}(\text{assoc})(x_A \rightarrow 0)$ corresponds to an enhancement of the probability that a HFB molecule at infinite dilution should be complexed with BEN, i.e., to the formation of structure in the solution. With further increase of BEN concentration, $\lim \phi_{C,A}(\text{assoc})(x_A \rightarrow 0)$ decreases because the entropy decrease produced by the formation of the complex is smaller than that occurring at lower BEN concentrations. Figure 1 also shows the results when the HFB molecule is changed by PFB. As it will be discussed in detail below, the pronounced decrease of $\lim \phi_{C,A}(\text{assoc})(x_A \rightarrow 0)$ can be associated with the decrease in quadrupole moment in going from HFB to PFB and shows the sensitivity of complex formation to changes in the charge distribution of the aromatic molecule. The association enthalpies, ΔH_{11} , and equilibrium constants, K_{11} , for the formation of the aromatic–aromatic complexes can be estimated using the TK association model described in the Appendix. The ΔH_{11} and K_{11} values, from a fit of eq A4 to the experimental $\lim \phi_{C,A}(\text{assoc})(x_A \rightarrow 0)$ data, are reported in Table 3. Clearly, the TK model is able to describe correctly the experimental behavior of $\lim \phi_{C,A}(\text{assoc})(x_A \rightarrow 0)$ in Figure 1 confirming the existence of the HFB–BEN and PFB–BEN complexes in the liquid solutions. The K_{11} and ΔH_{11} values for HFB–BEN are bigger than those for PFB–BEN, indicating that the former complex is more abundant and stronger. The magnitude of the ΔH_{11} values in Table 3 (average of -7.7 kJ mol⁻¹), when compared with those for complexes formed between molecules with an acidic hydrogen and a proton acceptor group (-18 to -20 kJ mol⁻¹),¹² indicate that the

TABLE 2: Infinite-Dilution Apparent Molar Heat Capacities, $\lim \phi_{C,A}(x_A \rightarrow 0)$, in $\text{J K}^{-1} \text{mol}^{-1}$ for A in Ternary Mixtures A + (*p* wt % B + *n*-heptane) at 298.15 K, as a Function of *p* (first column) for Each A–B Pair^a

HFB–MEN		HFB–BEN		HFB–TOL		NAP–HFB		PFB–MEN	
2.9	229.4 ± 2.2	5.1	221.7 ± 1.2	5.1	217.9 ± 1.1	4.9	197.8 ± 2.2	6.1	214.4 ± 1.7
5.1	233.7 ± 1.3	10.8	227.9 ± 0.4	9.9	234.2 ± 1.3	7.6	209.8 ± 1.6	11.2	210.8 ± 0.7
7.8	237.8 ± 2.0	14.8	232.5 ± 2.1	14.0	237.4 ± 1.3	10.8	215.2 ± 3.6	22.3	216.0 ± 0.7
10.2	243.1 ± 0.8	20.3	230.0 ± 1.2	23.0	242.1 ± 0.3	16.3	211.3 ± 1.3	32.4	221.4 ± 1.6
15.8	245.1 ± 0.8	22.7	231.0 ± 1.6	30.4	241.4 ± 1.5	23.9	216.5 ± 1.9	49.2	222.1 ± 1.1
20.0	251.5 ± 1.8	29.8	231.6 ± 0.4	39.7	235.5 ± 0.2	29.1	216.4 ± 5.5	65.3	226.6 ± 1.2
25.2	249.9 ± 0.7	35.8	227.1 ± 1.1			42.6	216.7 ± 1.2	74.5	221.9 ± 0.7
30.4	252.2 ± 1.3	49.7	225.8 ± 2.7			55.0	207.6 ± 2.0	82.0	225.8 ± 1.2
41.0	253.2 ± 2.8					57.9	209.8 ± 1.6		
50.1	250.9 ± 0.9								
67.2	248.0 ± 1.1								

PFB–BEN		HFB–FB		BEN–MEN		FB–MEN		TFB–MEN	
10.6	201.9 ± 1.1	5.9	216.6 ± 2.0	6.0	126.1 ± 0.2	10.8	142.2 ± 0.2	11.9	171.8 ± 1.2
25.8	204.5 ± 0.5	8.5	214.9 ± 0.5	11.3	127.1 ± 0.1	22.3	140.8 ± 2.3	23.2	170.1 ± 1.0
32.6	204.9 ± 1.5	10.7	216.6 ± 4.4	20.6	127.4 ± 0.1	40.1	141.9 ± 0.3	41.7	171.3 ± 0.7
44.9	207.1 ± 0.8	13.8	217.1 ± 1.5	38.4	127.9 ± 0.2				
57.4	205.7 ± 0.3	17.0	219.3 ± 3.4	53.8	128.6 ± 0.2				
67.0	205.5 ± 0.3	17.6	218.3 ± 0.7						
78.8	203.2 ± 1.0	20.9	219.1 ± 1.8						
		22.8	217.9 ± 0.7						
		29.4	214.8 ± 1.5						

^a At each *p* value, from a linear fit of the $\phi_{C,A}$ vs aromatic compound A concentration data.**Figure 1.** Experimental $\lim \phi_{C,A}(\text{assoc})(x^A \rightarrow 0)$ at 298.15 K for HFB (■) and PFB (□) in binary mixtures of BEN + *n*-C₇. Ω_2^* is the volume fraction of BEN in the binary BEN + *n*-C₇. Solid lines are a fit to the experimental data using the TK model, namely, eq A4, producing the complex formation parameters given in Table 3.

aromatic–aromatic complexes are quite weak. In obtaining eq A4, several assumptions have been made, namely, (i) the only associated species considered is the 1:1 complex $A_1B_1 = AB$, (ii) compounds A and B are both unable to self-associate, (iii) the enthalpy of mixing arises only from the formation of the AB species in solution, i.e. the TK model is an “athermal model”; as such, it deals only with the so-called chemical contributions to the thermodynamic properties, the physical contributions being all those arising from interactions in the system other than the association itself, and (iv) there are no volume changes due to association. For systems where association takes place through H bonds, it has been shown that the physical contribution to $\phi_C(\text{assoc})$ is negligible;¹¹ in the present work, the interactions giving rise to the formation of the complex AB are weak and hence assumption iii above must be regarded

TABLE 3: Enthalpy Changes, ΔH_{11} , and Equilibrium Constants, K_{11} , for the Formation of Aromatic–Aromatic Complexes at 298.15 K

complex A–B	r^a	r_1^b	$\Delta H_{11}/\text{kJ mol}^{-1}$	K_{11}
1 HFB–MEN	1.21	1.27	-10.8 ± 0.1	9.4 ± 0.6
2 HFB–BEN	0.77	1.27	-9.1 ± 0.9	7.0 ± 0.1
3 HFB–TOL	0.92	1.27	-8.8 ± 0.4	6.9 ± 2.2
4 NAP–HFB	1.05	1.34	-8.7 ± 0.2	16 ± 2
5 PFB–MEN	1.26	1.33	-8.6 ± 0.2	4.5 ± 0.7
6 PFB–BEN	0.81	1.33	-4.4 ± 0.2	4.5 ± 1.2
7 HFB–FB	0.81	1.27	-3.2 ± 0.2	14.4 ± 9.7
8 BEN–MEN ^c	1.56	1.65	0	-
9 FB–MEN ^c	1.49	1.57	0	-
10 TFB–MEN ^c	1.35	1.43	0	-

^a Molar ratio V_B/V_A . ^b Molar ratio V_I/V_A with I being *n*-heptane. ^c For these pairs, both terms in the right-hand side of eq 3 are equal within experimental error.

as a first approximation. Some of the compounds used here, e.g., benzene, have been found to form distinct, identifiable dimers in the pure liquid state³⁶ and, in the present work, are present at a relatively high concentration in the binaries B + I. On the other hand, assumption ii implies that the infinite dilution apparent heat capacity of A in the binary A + I should be equal to the heat capacity of pure A. Table 1 indicates, this is the case (maximum deviation is 7.4%), and hence, for the present systems, the effect of the self-association of A or B is negligible.

As the first nonvanishing central electric moment of HFB and BEN is the quadrupole moment, the electrostatic interaction of the HFB–BEN pair must be dominated by the quadrupole–quadrupole contribution. This conclusion can be assumed to remain true for all aromatic–aromatic pairs studied here where one or the two molecules have a nonzero, but very small, dipole moment. Because the quadrupole–quadrupole interaction is proportional to the product of the quadrupole moments of the molecules involved in the pair, it appears that when Q_A and Q_B have opposite signs and A and B are oriented in a face-to-face manner (molecular planes parallel) the interaction is favorable.¹⁴ Table 1 reports the quadrupole moments Q for all of the compounds studied in this work. HFB has a large positive quadrupole moment, whereas BEN has a large negative one, and hence, their quadrupole–quadrupole interaction is strong.

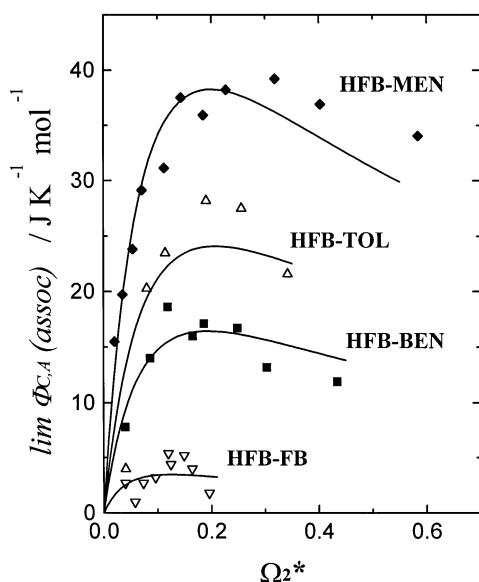


Figure 2. Experimental $\lim \phi_{C,A}(\text{assoc})(x_A \rightarrow 0)$ at 298.15 K for HFB in binary mixtures of B + *n*-C₇, with B being MEN (◆), TOL (△), BEN (■) and FB (▽). Ω_2^* is the volume fraction of B in the binaries B + *n*-C₇. Solid lines are a fit to the experimental data using the TK model, namely, eq A4, producing the complex formation parameters given in Table 3.

It is proposed here that this interaction provokes the formation of the HFB–BEN complex detected by the heat capacity measurements shown in Figure 1. The substitution of HFB by PFB produces, owing to the smaller positive quadrupole moment of PFB in Table 1, a weaker complex with BEN. As a consequence, $\lim \phi_{C,A}(\text{assoc})(x_A \rightarrow 0)$ in Figure 1 and the K_{11} and ΔH_{11} from the TK model fitting in Table 3 decrease in going from the HFB–BEN complex to the PFB–BEN case. The correspondence between the sign and magnitude of the quadrupole moment product $Q_A Q_B$ and the behavior of $\lim \phi_{C,A}(\text{assoc})(x_A \rightarrow 0)$ reflected in the K_{11} and ΔH_{11} parameters for the AB complex, suggests that by selecting aromatic molecules with different magnitudes and signs of their Q values, it is possible to obtain complexes of different strengths, i.e., of different enthalpies of association, ΔH_{11} . Furthermore, this correspondence can also be tested studying AB pairs whose A and B molecules have quadrupole moments of the same sign; as in this case, the face-to-face quadrupole–quadrupole interaction is unfavorable, and the complex should not be formed and hence be undetected by the heat capacity measurements (strictly speaking, when A and B have quadrupole moments of the same sign, an AB complex in the mutually perpendicular orientation will form, but the quadrupole–quadrupole interaction energy is very small,¹⁴ and the complex will most probably be undetectable by the heat capacity experiments). In what follows, the considerations outlined above are tested.

Figure 2 shows the experimental $\lim \phi_{C,A}(\text{assoc})(x_A \rightarrow 0)$ for several AB pairs with A being HFB ($Q > 0$) and B a series of aromatic compounds whose quadrupole moment is negative. As Q_B increases in magnitude (see Table 1) from FB to MEN, $\lim \phi_{C,A}(\text{assoc})(x_A \rightarrow 0)$ and, correspondingly, the enthalpies of association ΔH_{11} in Table 3 also increase. The adherence of eq A4 to the heat capacity data strongly suggests that the stoichiometry of these four complexes is 1:1. The strongest complex is HFB–MEN, a result which is consistent with the reported solid–liquid phase equilibria for this mixture that, as mentioned above, shows the formation of a complex which melts at a much higher temperature than the two pure components.

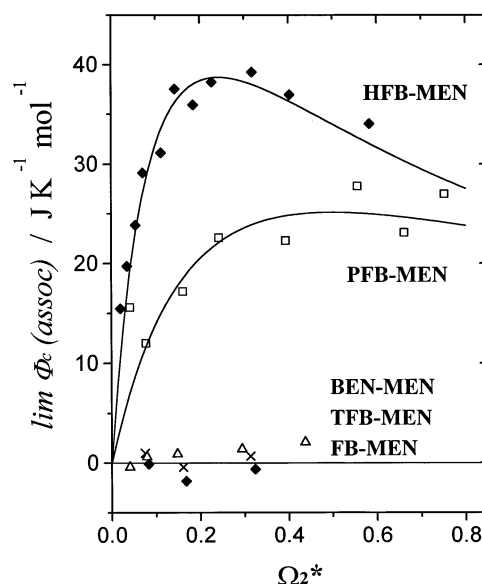


Figure 3. Experimental $\lim \phi_{C,A}(\text{assoc})(x_A \rightarrow 0)$ at 298.15 K for several aromatic compounds A, namely, HFB (◆), PFB (□), BEN (△), TFB (◆), and FB (×), in binary mixtures of MEN + *n*-C₇. Ω_2^* is the volume fraction of MEN in the binary MEN + *n*-C₇. Solid lines are a fit to the experimental data using the TK model, namely, eq A4, producing the complex formation parameters given in Table 3.

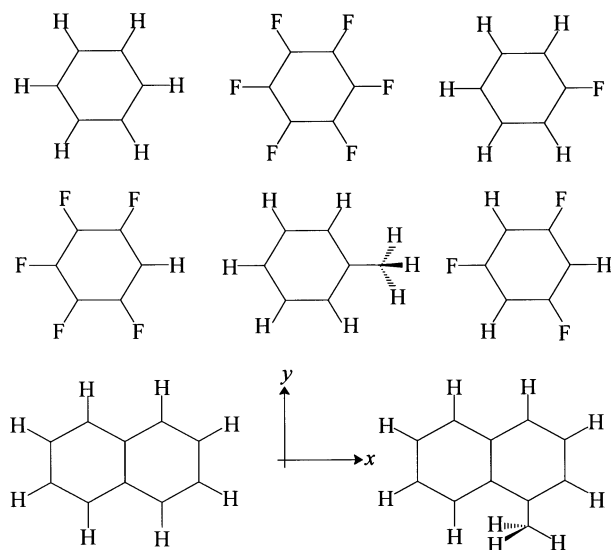
On the other hand, $\lim \phi_{C,A}(\text{assoc})(x_A \rightarrow 0)$ values for HFB–FB are small indicating a very weak complex. Because the value of K_{11} essentially depends on the Ω_2^* value where the maximum of $\lim \phi_{C,A}(\text{assoc})(x_A \rightarrow 0)$ occurs (see the Appendix), for HFB–FB, the fitting produced a large uncertainty on the equilibrium constant. Figure 3 shows the experimental $\lim \phi_{C,A}(\text{assoc})(x_A \rightarrow 0)$ for another set of AB pairs with B being MEN ($Q < 0$) and A a series of aromatic compounds whose quadrupole moment changes from positive to negative. When A is an aromatic with positive quadrupole moment, namely, HFB or PFB, Figure 3 shows that the complexes HFB–MEN and PFB–MEN are formed, with their K_{11} and ΔH_{11} being reported in Table 3. When A has a negative Q value (BEN and FB), $\lim \phi_{C,A}(\text{assoc})(x_A \rightarrow 0)$ values in Figure 3 are extremely small at all Ω_2^* concentrations; that is, both terms in the right-hand side of eq 3 are equal within experimental error and $\Delta H_{11} = 0$. These results support the conclusion that the formation of the AB complexes is determined by the sign of the $Q_A Q_B$ product. In Figure 3, $\lim \phi_{C,A}(\text{assoc})(x_A \rightarrow 0)$ values for TFB–MEN are very close to zero at all Ω_2^* concentrations; here, because of the small positive quadrupole moment of TFB (see Table 1), $Q_A Q_B < 0$ but very small and hence this system can be considered as a borderline case.

The electrostatic interaction energies, E_{elec} , of all of the dimers in Table 4 were calculated by eq 4 using the central electric moments of the molecules forming a given pair. The electrostatic energies using distributed electric moments, either from Stone or from AIM, are also given in Table 4. As the BEN–BEN pair has been a benchmark system³⁷ for theoretical calculations in the literature, it is also included in the table. For each dimer, the studied trajectories were determined by the set of Eulerian angles³⁸ that describe the relative orientation of the molecular pair and by the vector defined between the corresponding centers of mass. Based on symmetry considerations, only those trajectories considered as most likely were investigated and no numerical minimization of E_{elec} in terms of these degrees of freedom was performed. Reference frames for each complex are displayed in Figure 4, and the final molecular arrangements

TABLE 4: Electrostatic Interaction Energies (in kJ mol^{-1}) of Dimers of Aromatic Molecules Using Central and Distributed Multipole Moments

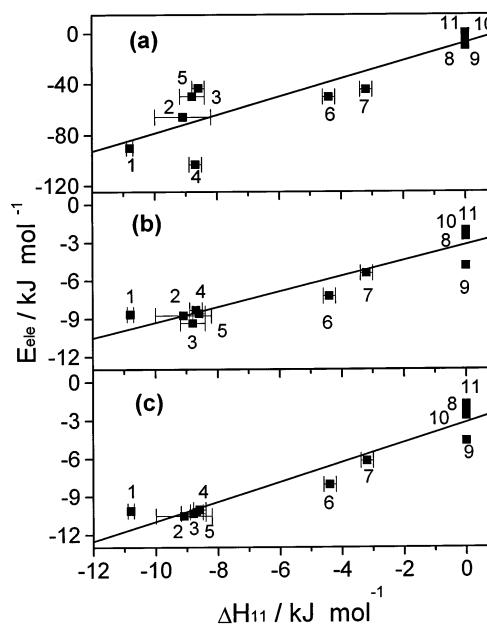
	Complex A–B	molecular arrangement		$E_{\text{elec}}(\text{CM})$	$E_{\text{elec}}(\text{Stone})$	$E_{\text{elec}}(\text{AIM})$
		(x, y, z)	(φ, θ, ψ)			
1	HFB–MEN	0.4, 0.4, 3.4	37, 0, 0	–90.09848	–8.64450	–10.10026
2	HFB–BEN	0.0, 0.0, 3.4	0, 0, 0	–65.84968	–8.73064	–10.50801
3	HFB–TOL*	0.6, 0.0, 3.4	0, 0, 0	–49.70538	–9.32005	–10.31823
4	NAP–HFB*	0.0, 0.0, 3.4	2, 0, 0	–103.02109	–8.31273	–10.18874
5	PFB–MEN	1.5, 0.0, 3.4	180, 0, 0	–43.36043	–8.57179	–10.02379
6	PFB–BEN	–0.3, 0.0, 3.4	0, 0, 0	–50.37939	–7.20920	–8.03386
7	HFB–FB*	0.2, 0.0, 3.4	0, 0, 0	–44.47920	–5.41535	–6.17471
8	BEN–MEN	0.0, 0.2, 5.35	0, 90, 0	–4.53551	–2.53579	–2.34923
9	FB–MEN	0.5, 0.5, 4.95	0, 90, 0	–9.99601	–4.84111	–4.62599
10	TFB–MEN	1.9, 0.0, 5.6	0, 90, 28	+0.26032	–2.27131	–2.65125
11	BEN–BEN	0.0, 0.0, 5.35	30, 90, 30	–3.00915	–2.06763	–1.76928

^a In all except the systems with asterisks, the molecular arrangement gives the orientation of the first molecule in a pair with respect to the second molecule fixed in the xy plane. The local origin of each molecule is located at the center of mass and oriented according to Figure 4.

**Figure 4.** Reference frame for each of the molecules for the calculation of E_{elec} . In each case, the origin of coordinates is located at the center of mass, with the z axis being perpendicular to the plane shown.

are given in Table 4. E_{elec} values for these final dimer geometries were compared to those obtained using the Orient program.³⁹ The two sets of E_{elec} agree within milihartrees (0.15 kJ mol^{-1}). This comparison provides support to our computer code, developed for the calculation of these energies. The van der Waals radii, necessary to define the short-range part of the Fowler-Buckingham potential, were taken from ref 40.

Several important observations can be made from the results in Table 4. When the interacting molecules have central quadrupole moments of opposite sign (systems 1–7) the face-to-face molecular arrangement is the most stable one, as concluded above from the enthalpy changes. In the case of systems 8–11, the molecules making up a given pair have central quadrupole moments of the same sign (except the borderline case TFB–MEN) and are arranged in a mutually perpendicular manner. For these pairs, the interaction energies are smaller than those for the face-to-face complexes. The E_{elec} values obtained with central moments are always bigger than those calculated with distributed moments. On the other hand, the comparison between Stone and AIM results shows that both sets of values are of the same order of magnitude. Similar results have been found for smaller systems.²⁸ In the present cases, the magnitude of the interaction energies agree well with the corresponding ΔH_{11} values, probably as a consequence of the improved convergence properties of the energy expansion in

**Figure 5.** Correlation between electrostatic interaction energies (E_{elec}) from Table 4 and the enthalpy changes, ΔH_{11} , from Table 3 for the formation of aromatic-aromatic complexes. Complexes are numbered according to the code used in Tables 3 and 4. E_{elec} values were calculated using central electric moments (a), and distributed electric moments either from Stone (b) or from AIM (c). Correlation coefficients are 0.8855 (a), 0.9431 (b), and 0.9609 (c).

terms of distributed moments. Using the data in Tables 3 and 4, Figure 5 shows empirical correlations between E_{elec} and ΔH_{11} . Even though the points on each of the panels in Figure 5 do not necessarily have to lie on a straight line, a least-squares linear fitting can be used to assess the relation between E_{elec} and ΔH_{11} . The correlation coefficients indicate that the best fitting is obtained when either of the two sets of distributed moments is used. The results in Figure 5 show that the electrostatic contribution to the interaction energy is mainly responsible for the changes in association enthalpies of the complexes studied.

Acknowledgment. We thank Dr. Ángel Piñero and Dr. Ernesto Carrillo-Nava for their useful comments. This work was supported by the Consejo Nacional de Ciencia y Tecnología de México (CONACyT, grant 27986-E).

Appendix. Association Model

The original Treszczanowicz and Kehiaian (TK) model¹³ was developed to study association (self- and cross association) in

liquid mixtures, the most common case being that where association takes place through the formation of H bonds. This model has been extended a number of times,¹¹ in order to study different types of associated mixtures. In particular, the extension to ternary mixtures¹² of the type A + (B + I) is relevant for the present work; here, A (component 1) and B (component 2) are substances which can form a complex or associated species AB in solution and I is an inert solvent (component 3). According to this extension, the associational part of the apparent molar heat capacity of compound A is given by

$$\phi_C(\text{assoc}) = \left[\frac{\Delta H_{11}}{T} \right] \frac{\phi_2 \phi_A X / r \phi_1}{R(1 + \phi_2 X / r)} \quad (\text{A1})$$

where

$$X = \frac{[r/(r+1)]K_{11}}{[[r/(r+1)]K_{11}\phi_A + 1]^2}$$

and

$$\phi_1 = x_1/(x_1 + rx_2 + r_1x_3) \quad (\text{A2})$$

In eqs A1 and A2, K_{11} and ΔH_{11} are the volumetric equilibrium constant and the enthalpy change for the formation of species $A_1B_1 = AB$ (1:1 complex); ϕ_i and x_i ($i = 1-3$) are the volume and mol fractions of each component, r and r_1 are the ratios of molar volumes V_2/V_1 and V_3/V_1 , respectively, and ϕ_A is the volume fraction of compound A in solution that is in the form of monomers, i.e., not forming any complex AB. This fraction is obtained as the closest root to zero of the mass balance equation

$$\phi_A - \phi_1 + \frac{\phi_2 - \phi_A K_{11}/(r+1)}{[r/(r+1)]K_{11}\phi_A + 1} = 0 \quad (\text{A3})$$

From eqs A1 to A3, the infinite-dilution limit of the associational part of the apparent molar heat capacity of compound A in the ternary mixture, i.e., $\lim \phi_C(\text{assoc})(x_1 \rightarrow 0)$ is given by

$$\lim \phi_C(\text{assoc})(x_1 \rightarrow 0) = \left[\frac{\Delta H_{11}}{T} \right] \frac{K_{11}\Omega_2^*/(1+r)}{R[1 + (K_{11}\Omega_2^*)/(1+r)]^2} \quad (\text{A4})$$

This limit corresponds to the situation where an isolated A molecule is surrounded by a B + I binary mixture and is forming a complex with B. This limit can then be regarded as the contribution to the heat capacity due to the formation of the AB species. In eq A4, $\Omega_2^* = x_2'/(x_2' + (V_3/V_2)x_3')$, with $x_2' + x_3' = 1$; as such, Ω_2^* is the volume fraction of B in the mixture B + I. Equation A4 can be used to obtain the parameters K_{11} and ΔH_{11} from a fit to the experimental values of $\phi_C(\text{assoc})(x_1 \rightarrow 0)$ from eq 3 in the text. From eq A4, it is easy to show that the maximum value for $\phi_C(\text{assoc})(x_1 \rightarrow 0)$ is given by $\Delta H_{11}^2/4RT^2$ occurring at $\Omega_2^* = (1+r)/K_{11}$. Note that within the framework of the present association model, eq A4 can be used to characterize any AB interaction from heat capacity measurements; this has been done previously for alcohol-proton acceptor complexes¹² and for alcohol-reverse micelle interactions.⁴¹

References and Notes

- (1) (a) Hunter, C. A.; Sanders, J. K. M. *J. Am. Chem. Soc.* **1990**, *112*, 5525. (b) Hunter, C. A. *Angew. Chem., Int. Ed. Engl.* **1993**, *32*, 1584. (c) Weck, M.; Dunn, A. R.; Matsumoto, K.; Coates, G. W.; Lobkovsky, E. B.; Grubbs, R. H. *Angew. Chem., Int. Ed. Engl.* **1999**, *38*, 2741. (d) Chelli, R.; Gervasio, F. L.; Procacci, P.; Schettino, V. *J. Am. Chem. Soc.* **2002**, *124*, 6133. (e) Gervasio, F. L.; Chelli, R.; Procacci, P.; Schettino, V. *Proteins: Struct., Funct., Genet.* **2002**, *48*, 117.
- (2) Ortholand, J.-Y.; Slawin, A. M. Z.; Spencer, N.; Stoddart, J. F.; Williams, D. J. *Angew. Chem., Int. Ed. Engl.* **1989**, *28*, 1394, and references therein.
- (3) Burkley, S. K.; Petsko, G. A. *Adv. Protein Chem.* **1988**, *39*, 125.
- (4) Patrick, C. R.; Prosser, G. S. *Nature* **1960**, *187*, 1021.
- (5) Griffith, G.; Jackson, P. R.; Kenyon-Blair, E.; Morcom, K. W. *J. Chem. Thermodyn.* **1983**, *15*, 1001.
- (6) Duncan, W. A.; Swinton, F. L. *Trans. Faraday Soc.* **1966**, *62*, 1082.
- (7) (a) Overell, J. S. W.; Pawley, G. S. *Acta Cryst.* **1982**, *B38*, 1966. (b) Duer, M. J. *J. Chem. Soc., Faraday Trans.* **1993**, *89*, 823.
- (8) Neelakandan, M.; Pant, D.; Quitevis, E. L. *Chem. Phys. Lett.* **1997**, *265*, 283.
- (9) (a) Fenby, D. V.; McLure, I. A.; Scott, R. L. *J. Phys. Chem.* **1966**, *70*, 602. (b) Duncan, W. A.; Sheridan, J. P.; Swinton, F. L. *Trans. Faraday Soc.* **1966**, *62*, 1090. (c) Duncan, W. A.; Swinton, F. L. *J. Phys. Chem.* **1966**, *70*, 2417. (d) Gaw, W. J.; Swinton, F. L. *Nature* **1966**, *212*, 283. (e) Fenby, D. V.; Scott, R. L. *J. Phys. Chem.* **1967**, *71*, 4103. (f) Gaw, W. J.; Swinton, F. L. *Trans. Faraday Soc.* **1968**, *64*, 637. (g) Gaw, W. J.; Swinton, F. L. *Trans. Faraday Soc.* **1968**, *64*, 2023. (f) Powell, R. J.; Swinton, F. L. *J. Chem. Thermodyn.* **1970**, *2*, 87. (h) Powell, R. J.; Swinton, F. L.; Young, C. L. *J. Chem. Thermodyn.* **1970**, *2*, 105.
- (10) (a) Bartsch, E.; Bertagnolli, H.; Chieux, P. *Ber. Bunsen-Ges. Phys. Chem.* **1986**, *90*, 34. (b) Cabaco, M. I.; Danten, Y.; Besnard, M.; Guissani, Y.; Guillot, B. *J. Phys. Chem. B* **1998**, *102*, 10712.
- (11) (a) Costas, M.; Patterson, D. *J. Chem. Soc., Faraday Trans. 1* **1985**, *81*, 635. (b) Costas, M.; Patterson, D. *J. Chem. Soc., Faraday Trans. 1* **1985**, *81*, 655. (c) Andreoli-Ball, L.; Patterson, D.; Costas, M.; Caceres-Alonso, M. *J. Chem. Soc., Faraday Trans. 1* **1988**, *84* (11), 3991. (d) Perez-Casas, S.; Trejo, L. M.; Costas, M. *J. Chem. Soc., Faraday Trans. 1991*, *87* (11), 1733. (e) Trejo, L. M.; Perez-Casas, S.; Patterson, D.; Costas, M. *J. Chem. Soc., Faraday Trans.* **1991**, *87* (11), 1739. (f) Salcedo, D.; Costas, M. *J. Chem. Soc., Faraday Trans.* **1997**, *93* (21), 3781. (g) Figueroa-Gerstenmaier, S.; Cabañas, A.; Costas, M. *Phys. Chem. Chem. Phys.* **1999**, *1*, 665.
- (12) (a) Costas, M.; Yao, Z.; Patterson, D. *J. Chem. Soc., Faraday Trans. 1* **1989**, *85*, 2211. (b) Deshpande, D. D.; Patterson, D.; Andreoli-Ball, L.; Costas, M.; Trejo, L. M. *J. Chem. Soc., Faraday Trans.* **1991**, *87*, 1133.
- (13) Kehiaian, H.; Treszczanowicz, A. J. *Bull. Acad. Chim. Fr.* **1969**, *5*, 1561.
- (14) (a) Brown, N. M. D.; Swinton, F. L. *J. Chem. Soc. Chem. Commun.* **1974**, 770. (b) Hernandez-Trujillo, J.; Costas, M.; Vela, A. *J. Chem. Soc., Faraday Trans.* **1993**, *89*, 2441.
- (15) Fowler, P. W.; Buckingham, A. D. *Chem. Phys. Lett.* **1991**, *176*, 11.
- (16) Price, S. L.; Stone, A. J. *J. Chem. Phys.* **1987**, *86*, 2859.
- (17) Hernandez-Trujillo, J.; Colmenares, F.; Cuevas, G.; Costas, M. *Chem. Phys. Lett.* **1997**, *265*, 503.
- (18) Stone, A. J. *Chem. Phys. Lett.* **1981**, *83*, 233.
- (19) Stone, A. J.; Alderton, M. *Mol. Phys.* **1985**, *56*, 1047.
- (20) Bader, R. F. W. *Atoms in Molecules. A Quantum Theory*; Clarendon: Oxford, 1990.
- (21) Buckingham, A. D.; Fowler, P. W. *J. Chem. Phys.* **1983**, *79*, 6426.
- (22) Buckingham, A. D.; Fowler, P. W. *Can. J. Chem.* **1985**, *63*, 2018.
- (23) Price, S. L. *Chem. Phys. Lett.* **1985**, *114*, 359.
- (24) Jansen, G.; Hättig, C.; Hess, B. A.; Ángyán, J. G. *Mol. Phys.* **1996**, *88*, 69.
- (25) (a) Picker, P.; Leduc, P. A.; Philip, P. R.; Desnoyers, J. E. *J. Chem. Thermodyn.* **1971**, *3*, 631. (b) Fortier, J. L.; Benson, G. C. *J. Chem. Thermodyn.* **1976**, *8*, 411.
- (26) Riddick, J. A.; Bunger, W. B.; Sakano, T. K. *Organic Solvents: Physical Properties and Methods of Purification, Techniques in Chemistry*; Wiley-Interscience: New York, 1986.
- (27) Kosov, D. S.; Popelier, P. L. A. *J. Phys. Chem. A* **2000**, *104*, 7339.
- (28) Popelier, P. L. A.; Joubert, L.; Kosov, D. S. *J. Phys. Chem. A* **2001**, *105*, 8254.
- (29) Hernández-Trujillo, J.; Vela, A. *J. Phys. Chem.* **1996**, *100*, 6524.
- (30) George, P.; Bock, C.; Stezowski, J. J.; Hildenbrand, T.; Glusker, J. P. *J. Phys. Chem.* **1988**, *92*, 5656.
- (31) (a) Almenningsen, A.; Bastiansen, O.; Seip, R.; Seip, H. *Acta Chem. Scand.* **1964**, *18*, 2115. (b) Nygaard, L.; Bojensen, Y.; Pederson, T.; Rastrup-Andersen, J. *J. Mol. Struct.* **1968**, *2*, 209. (c) Pawley, G. S.; Yeats, E. A. *Acta Crystallogr. B* **1969**, *25*, 2009. (d) Doraiswamy, S.; Charma, D. D. *Pramana* **1974**, *2*, 219. (e) Tamagawa, K.; Iijima, T.; Kimura, M. *J. Mol. Struct.* **1976**, *30*, 243. (f) Amir-Ebrahimi, V.; Choplin, A.; Demaison, J.; Roussy, G. *J. Mol. Spectrosc.* **1981**, *89*, 42. (g) Almenningsen, A.; Hargittai, Y.; Bruvonn, J.; Domenicano, A.; Samdal, S. *J. Mol. Struct.* **1984**, *116*, 199.
- (32) Amos, R. D.; Rice, J. E. *Cadpac: The Cambridge Analytical Derivatives Package. Issue 5.0*; University of Cambridge: Cambridge, 1991.

- (33) Biegler-König, F. W.; Badern, R. F. W.; Tang, T.-H. *J. Comput. Chem.* **1982**, *3*, 317.
- (34) Frisch, M. J.; Trucks, G. W.; Schlegel, H. B.; Gill, P. M. W.; Johnson, B. G.; Robb, M. A.; Cheeseman, J. R.; Keith, T.; Petersson, G. A.; Montgomery, J. A.; Raghavachari, K.; Al-Laham, M. A.; Zakrzewski, V. G.; Ortiz, J. V.; Foresman, J. B.; Cioslowski, J.; Stefanov, B. B.; Nanayakkara, A.; Challacombe, M.; Peng, C. Y.; Ayala, P. Y.; Chen, W.; Wong, M. W.; Andres, J. L.; Replogle, E. S.; Gomperts, R.; Martin, R. L.; Fox, D. J.; Binkley, J. S.; Defrees, D. J.; Baker, J.; Stewart, J. P.; Head-Gordon, M.; Gonzalez, C.; Pople, J. A. *Gaussian 94*, revision D.4; Gaussian, Inc.: Pittsburgh, PA, 1995.
- (35) Buckingham, A. D. *Basic theory of intermolecular forces: applications to small molecules*, in *Intermolecular Interactions: from diatomics to polymers*, Ed. Pullman, B. John Wiley: New York **1978**.
- (36) (a) Cox, E. G.; Cruickhank, D. W. J.; Smith, J. A. S. *Proc. R. Soc.* **1958**, 247, 1. (b) Narten, A. H. *J. Chem. Phys.* **1977**, *67*, 2102. (c) Clement, C. *J. Chim. Phys.* **1978**, *75*, 747. (d) Cabaco, M. I.; Danten, Y.; Besnard, M.; Guissani, Y.; Guillot, B. *J. Phys. Chem. B* **1997**, *101*, 6977.
- (37) (a) Hobza, P.; Selzle, H. L.; Schlag, E. W. *J. Am. Chem. Soc.* **1994**, *116*, 3500. (b) Hobza, P.; Selzle, H. L.; Schlag, E. W. *J. Phys. Chem.* **1996**, *100*, 18790. (c) Tsuzuki, S.; Uchimaru, T.; Matsumara, K.; Mikami, M.; Tanabe, K. *Chem. Phys. Lett.* **2000**, *319*, 547.
- (38) Goldstein, H.; *Classical Mechanics*, 2nd ed.; Addison-Wesley: Reading, MA, 1980.
- (39) Stone, A. J.; Dullweber, A.; Hodges, M. P.; Popelier, P. L. A.; Wales, D. J. *Orient, A program for Studying Interactions between Molecules*, version 3.2; University of Cambridge: Cambridge, U.K., 1995.
- (40) Pauling, L. *The Nature of the Chemical Bond*, 3rd ed.; Cornell University Press: Ithaca, NY, 1960.
- (41) Perez-Casas, S.; Castillo, R.; Costas, M. *J. Phys. Chem. B* **1997**, *101*, 7043.
- (42) CDATA, *Database of Thermodynamic and Transport Properties for Chemistry and Engineering*; Department of Physical Chemistry. Institute for Chemical technology (distributed by FIZ Chemie GmbH Berlin): Prague, 1991.